

High-throughput screening and hit validation of extracellular-related kinase 5 (ERK5) inhibitors.

Stephanie May Myers, Ruth Helen Bawn, Louise C Bisset, Timothy J. Blackburn, Betty Cottyn, Lauren Molyneux, Ai-Ching Wong, Celine Cano, William Clegg, Ross W. Harrington, Hing Leung, Laurent Rigoreau, Sandrine Vidot, Bernard Thomas Golding, Roger John Griffin, Tim Hammonds, David R. Newell, and Ian Robert Hardcastle

ACS Comb. Sci., **Just Accepted Manuscript** • DOI: 10.1021/acscombsci.5b00155 • Publication Date (Web): 11 Jul 2016

Downloaded from <http://pubs.acs.org> on July 12, 2016

Just Accepted

"Just Accepted" manuscripts have been peer-reviewed and accepted for publication. They are posted online prior to technical editing, formatting for publication and author proofing. The American Chemical Society provides "Just Accepted" as a free service to the research community to expedite the dissemination of scientific material as soon as possible after acceptance. "Just Accepted" manuscripts appear in full in PDF format accompanied by an HTML abstract. "Just Accepted" manuscripts have been fully peer reviewed, but should not be considered the official version of record. They are accessible to all readers and citable by the Digital Object Identifier (DOI®). "Just Accepted" is an optional service offered to authors. Therefore, the "Just Accepted" Web site may not include all articles that will be published in the journal. After a manuscript is technically edited and formatted, it will be removed from the "Just Accepted" Web site and published as an ASAP article. Note that technical editing may introduce minor changes to the manuscript text and/or graphics which could affect content, and all legal disclaimers and ethical guidelines that apply to the journal pertain. ACS cannot be held responsible for errors or consequences arising from the use of information contained in these "Just Accepted" manuscripts.



1
2
3
4
5
6
7
8
9
10
11
12
13
14
15
16
17
18
19
20
21
22
23
24
25
26
27
28
29
30
31
32
33
34
35
36
37
38
39
40
41
42
43
44
45
46
47
48
49
50
51
52
53
54
55
56
57
58
59
60

High-throughput screening and hit validation of extracellular-related kinase 5 (ERK5) inhibitors.

Stephanie M. Myers¹, Ruth H. Bawn¹, Louise C. Bisset³, Timothy J. Blackburn¹, Betty Cottyn¹, Lauren Molyneux¹, Ai-Ching Wong⁴, Celine Cano¹, William Clegg², Ross. W. Harrington², Hing Leung⁵, Laurent Rigoreau⁴, Sandrine Vidot,¹ Bernard T. Golding¹, Roger J. Griffin¹, Tim Hammonds⁴, David R. Newell³, Ian R. Hardcastle^{1*}

¹ Newcastle Cancer Centre, Northern Institute for Cancer Research and School of Chemistry, Bedson Building, Newcastle University, Newcastle upon Tyne, NE1 7RU, UK

² School of Chemistry, Bedson Building, Newcastle University, Newcastle upon Tyne, NE1 7RU, UK

³ Newcastle Cancer Centre, Northern Institute for Cancer Research, Paul O’Gorman Building, Medical School, Framlington Place, Newcastle University, Newcastle upon Tyne, NE2 4HH, UK

⁴ Cancer Research Technology Ltd, Discovery Laboratories, Wolfson Institute for Biomedical Research, The Cruciform Building , Gower Street, London, WC1E 6BT, UK

⁵ The Beatson Institute for Cancer Research, Garscube Estate, Switchback Road, Bearsden, Glasgow G61 1BD, UK

Abstract

The extracellular-related kinase 5 (ERK5) is a promising target for cancer therapy. A high-throughput screen was developed for ERK5, based on the IMAP FP Progressive Binding System, and used to identify hits from a library of 57,617 compounds. Four distinct chemical series were evident within the screening hits. Resynthesis and re-assay of the hits demonstrated that one series did not return active compounds, whereas three series returned active hits. Structure-activity studies demonstrated that the 4-benzoylpyrrole-2-carboxamide pharmacophore had excellent potential for further development. The minimum kinase binding pharmacophore was identified, and key examples demonstrated good selectivity for ERK5 over p38 α kinase.

INTRODUCTION

The extracellular-related kinase 5 (ERK5), also known as Big Map Kinase (BMK1), is a 816 amino acid protein kinase that forms part of a non-canonical MAP kinase pathway in cells.¹ Extracellular stimulation, in the form of growth factors, such as epidermal growth factor (EGF), nerve growth factor (NGF), vascular endothelium growth factor (VEGF), and fibroblast growth factor-2 (FGF-2), initiates a signalling cascade from the cell surface to nuclear transcription factors via ERK5.² Unlike the linear canonical Ras/Raf/MEK/ERK pathway, the ERK5 signalling cascade occurs independently of Raf.³ ERK5 is activated specifically by MEK5, which is in turn activated by MEKK2/3.^{1a, 4}

ERK5 is structurally different from the other members of the ERK sub-families. A unique loop-12 structure and extended C-terminal domain (~400 amino acids) gives ERK5 its characteristic structure.^{2, 4} The C-terminal extension harbours nuclear localisation and export sequences, two proline-rich domains, a transcriptional activating domain, and MEF2 interacting region. The large C-terminal unique to ERK5 is auto-phosphorylated at multiple sites, resulting in an increase in transcriptional activity.⁵

Phosphorylation of ERK5 results in activation of a number of transcription factors including MEF2, c-Myc, c-Jun, c-Fos, Fra-1, and NF κ B.⁶ ERK5 also phosphorylates and activates p90 RSK, also involved in signal transduction.⁷ An increasing body of mechanistic data indicates that ERK5 plays a key role in tumor biology, i.e. cell proliferation and survival, invasion and metastasis, and angiogenesis.⁸

Expression of ERK5 is significantly up-regulated in advanced prostate cancer and has been identified as an independent prognostic biomarker for aggressive disease.⁹ ERK5 is over-expressed in 20% of breast cancer patients and its expression is an independent prognostic biomarker for reduced disease-free survival.¹⁰ In hepatocellular carcinoma (HCC), ERK5 overexpression has been reported, associated with gene amplification at the 17p11 chromosome fragment, harboring the MAPK7 gene.¹¹ High levels of ERK5 were found to correlate with more aggressive and metastatic stages in fresh samples from human clear cell renal cell carcinoma.¹²

To date, three small-molecule inhibitors of the MEK5/ERK5 pathway have been described. The indolinone based inhibitors, BIX02188 (**1a**) and BIX02189 (**1b**), are dual inhibitors of the MEK5/ERK5 cascade. Both compounds inhibit MEK5 with nanomolar potency, whereas modest activity was reported for ERK5.¹³ Benzo[e]pyrimido-[5,4-

b)diazepine-6(11*H*)-one (XMD8-92, **2**) is a potent ERK5 inhibitor which exhibits anti-proliferative and anti-angiogenic effects on HeLa cells in mouse xenograft models.¹⁴ An X-ray crystal structure of **2** bound to ERK5 shows the inhibitor bound to the Met140 in the kinase hinge *via* a pair of hydrogen bonds from the aniline and pyrimidine nitrogens, and an additional water-bridged hydrogen bond from the diazepinone carbonyl to Asp200 and Glu102 in the DFG loop.¹⁵ However, some of the *in vivo* activity of **2** has been attributed to off-target activities e.g. inhibition of doublecortin-like kinase 1 (DCLK-1) in pancreatic cancer.¹⁶ Inhibition of ERK5 or siRNA knockdown has been shown to inhibit the growth of HCC cell lines, *in vitro* and *in vivo*.¹⁷ ERK5 signalling has been shown to be essential for chemically induced carcinogenesis in skin by *erk5* gene deletion or ERK5 inhibition (with **2**).¹⁸ The combination of doxorubicin and either *erk5* gene deletion or ERK5 inhibition (with **2**) was found to be additive in inflammation-driven tumour models. Thus, pharmacological inhibition of ERK5 may provide an opportunity for the treatment of inflammation-driven, invasive or metastatic cancers where ERK5 is deregulated. Given the strong link between ERK5 mediated signalling and malignancy, there remains a strong need to develop selective tool molecules to fully elucidate the effect of ERK5 inhibition *in vivo*. For this reason, we sought to discover novel ERK5 inhibitory chemotypes through high-throughput screening as chemical tools and for development as therapeutic agents.

In this paper, we describe the development of a high-throughput screening assay for ERK5 inhibition based on the IMAP FP format that was used to identify four discrete series of hit molecules. Validation of each series was attempted by resynthesis and retesting of selected members from each series. Preliminary structure activity studies were obtained resulting in the identification of one series for further optimisation.

DEVELOPMENT AND EXECUTION OF ERK5 IMAP SCREEN

Assay development

The discovery of kinase inhibitors using high-throughput screening is well established.¹⁹ In our case, expression of active ERK5 protein required co-expression of MEK5. The screen was developed using the IMAP format (Molecular Devices) that relies on the high specificity interaction of phospho groups on a fluorescently tagged peptide with M³⁺ containing nanoparticles. The IMAP format was chosen as a robust and efficient method of determining kinase activity using a 'mix-and-measure' format with a non-radioactive, fluorescence output.

Preliminary experiments to determine a suitable peptide substrate for the IMAP FP assay used a commercial source of the enzyme and were based on sequence of the natural substrate of ERK5, and were augmented with a substrate finder kit. Five peptide sequences were designed based around the reported site of phosphorylation of MEF2C by ERK5, with the expected serine phosphorylation site highlighted in red (Table 1).¹ The peptides were tested using the IMAP FP Progressive Binding System (Molecular Devices) in the absence and presence of ERK5 (Carna Biosciences).

The IMAP FP substrate finder kit for serine/threonine kinases plate 2 (Molecular Devices) covering CMGC, CK1, STE, and TKL portions of the kinome was used to identify potential peptide substrates phosphorylated by ERK5. The FAM-EGFR-derived peptide (LVEPLTPSGEAPNQK-5FAM-COOH) proved optimal.

Kinetic studies determined the ERK5 K_M^{app} to be 300 μ M. Ideally, kinase screens are run with the ATP concentration equal to the K_M , however, in this case the IMAP format did not return acceptable results at a high ATP concentration (300 μ M), presumably due to interference of ATP with the interaction of the phospho peptide with the metal nanoparticles. For this reason, the HTS assay was run at the maximum acceptable ATP concentration (100 μ M) to allow 'mix-and-measure' determinations.

High-throughput Screening for ERK5 inhibitors

To identify inhibitors of ERK5 the IMAP HTS assay was set up and a library of 57,617 small molecules was screened (final DMSO concentration of 4% and a total reaction volume of 40 μ L). The library was composed of a 48,479 member diverse library and a 9136 member kinase focussed library, both libraries were sourced from commercial vendors. Z' factors for each plate were calculated using Equation 2, and were typically 0.6-0.8. Plates with Z' factors below 0.4 were re-screened (Supporting Information).

HTS Results

The HTS assay returned 245 active compounds (0.5 % hit rate), i.e. >50% inh at 30 μ M, from the 57,617 member library. Active compounds (245) showing >50% inhibition in the screen were resupplied from stock or commercial vendors and retested at 30, 10 and 3.3 μ M. 71 active compounds, giving >30% mean inhibition, were treated as confirmed hits (0.10% overall hit-rate) and assayed over a full IC_{50} range. IC_{50} determinations required a two stage process whereby the reaction occurred initially in the absence of the IMAP reagent, followed by subsequent addition of the IMAP reagent, to allow the K_M concentration of ATP to be used.

The hit compounds produced inhibition curves with IC_{50} values ranging from 0.6 to 76 μ M (1 compound >120 μ M). Confirmed hits were clustered according to common structures, revealing four promising chemical series. SAR around the hits was expanded by assaying related in-house compounds and close analogues from commercial suppliers. From these results, four compound series were selected for validation by resynthesis prior to progressing to hit-to-lead studies: 2-amino-*N,N*-alkylbenzo[d]thiazole-6-sulfonamides (Table 2, **3a-c**); 4-substituted-2-(substitutedthio)-6-phenylnicotinonitriles (Table 3, **4a,b**); 4-amino-2-(arylamino)pyrimidine-5-carbonitriles (Table 5, **5a-c**); and 4-aryl-*N*-alkyl-1*H*-pyrrole-2-carboxamides (Table 6, **6a-e**).

SYNTHESIS

Benzothiazole Series 3

Numerous methods have been described for the synthesis of benzothiazoles.²⁰ For the synthesis of compounds **3a,b** and analogues, we used the reported reaction of anilines with potassium thiocyanate-copper(II) sulfate (Scheme 1).²¹ The required 4-aminophenylsulfonamides (**7a-c**) were prepared by reduction of the corresponding nitro compounds (**8a-c**). The nitro precursors were obtained by coupling the relevant amine with 4-nitrobenzenesulfonyl chloride. The 5-sulfonamide isomer **9a**, was prepared *via* the same method (Scheme 2). Thus, 3-nitrobenzenesulfonyl chloride was reacted with pyrrolidine or *N*-methylethylamine, and the resulting sulfonamides **10a,b** were reduced to the

respective anilines **11a,b** (Scheme 2). Reactions of **11a,b** with potassium thiocyanate-copper(II) sulfate gave in each case, besides the desired 5-substituted benzothiazole **9a,b**, a significant quantity of a thiocyanatobenzene (**12a,b**).

Nicotinonitrile Series 4

The first synthetic approach considered for the synthesis of 3-cyanopyridines was based on the route reported by Shestopalov et al.²² For example, 4-fluorochalcone **13a**, prepared *via* Claisen-Schmidt condensation of acetophenone with 4-fluorobenzaldehyde, was treated with elemental sulfur and morpholine in ethanol at reflux, followed by malononitrile, to give pyridinethione **14a** in moderate yield (Method A, Scheme 3). Isolation of the intermediate pyridinethiones **14** required extensive purification, attributed to the propensity of this intermediate to tautomerise, and its readiness to oxidise under atmospheric conditions.

Consideration of the likely mechanism of the one-pot sequence of the cyclisation reaction prompted the replacement of the sulfur and malononitrile with 2-cyanothioacetamide for the Michael addition in an alternative route (Method B, Scheme 3). Reactions were performed under nitrogen to avoid oxidative side-reactions. The crude intermediate **14** was used directly in the alkylation step, to avoid a lengthy purification, giving cyanopyridines **15a-k**. Method B allowed isolation of **15a** in an improved 54% yield over 2 steps. Deprotection with TFA gave acids **4a-k** in near quantitative yield (99%). The carboxamide **17** was prepared from **4a** by a HBTU-mediated coupling with *p*-methoxybenzylamine giving amide **16**, which was deprotected with TFA.

Further variations to the thioether group were introduced *via* alkylation of **14a** (Schemes 4-7). The acetamide derivatives **31** and **32** were prepared by the alkylation of **14a** and **14g**, respectively, with bromoacetamide **30** which was obtained by reaction of aminoacetone hydrochloride **29** with bromoacetylchloride (Scheme 8).²³

Cyanopyrimidine Series 5

A small series of 4-amino-2-anilinopyrimidine-5-carbonitriles (**5a-c**) were prepared by the reaction of the appropriate aniline with chloropyrimidine (**33**) at 100 °C in DMF (Scheme 9).²⁴

4-Benzoylpyrrole-2-carboxamide Series 6

A selection of 4-benzoylpyrrole-2-carboxamides were prepared by Friedel-Crafts acylation of methyl 1*H*-pyrrole-2-carboxylate (**34**) with a substituted benzoyl chloride giving pyrrole (**35**). Hydrolysis of the methyl ester with lithium hydroxide gave carboxylic acid **36** that was coupled with the appropriate amine using CDI to give the desired carboxamides (**6a-r**) (Scheme 10). The *N*-methyl derivative **6m** was prepared by methylation of ester **35a**, followed by hydrolysis and coupling with 3-pyridylmethylamine (Scheme 11).

2-Substituted-4-benzoylpyrrole derivatives

The alkene derivative **40** was prepared by aldol condensation of ketone **39** and isonicotinaldehyde (Scheme 12). Selective reduction was achieved by refluxing alkene **40** in aqueous ethanol with indium metal and ammonium

chloride giving alkane **41** in moderate yield.²⁵ The cyclopropyl analogue **42** was prepared by a Corey Chaykovsky reaction.²⁶ Thus, alkene **40** was reacted with trimethylsulfoxonium iodide and potassium *tert*-butoxide giving **42** in 12% yield.²⁷ Diketone **44** was prepared *via* a Claisen condensation between 1-(1*H*-pyrrol-2-yl)ethanone and methyl isonicotinate diketone **43** (Scheme 13). Friedel-Crafts acylation with 2,3-dichlorobenzoyl chloride gave **44**.

DISCUSSION

Selected examples of the HTS hits in the benzothiazole series (**3a**, **3b**, **3i**) were synthesised and re-assayed. The ERK5 inhibitory activity for the resynthesized benzothiazoles were 1000-fold lower than for the library material (Table 2). Comparison of the ¹H-NMR and LCMS spectra of the resynthesized and screened samples of **3a** suggested that the library material was the 5-sulfonamide **9a**, so authentic samples of isomers **9a** and **9b** were prepared. In order to eliminate the possibility of mis-identification of the compounds by spectroscopic methods, the identity of isothiocyanate **12a** and benzothiazoles **3a** and **3i** were elucidated by small-molecule X-ray crystallography (Figures 1-3).

The assay results for these isomers also failed to replicate the initial IC₅₀ values from the screening samples. Interestingly, the isothiocyanate side-product **12a** showed 10-fold greater potency than the benzothiazole, although this result was not replicated for the analogue **12b**. Time-dependent enzyme inactivation by isothiocyanates, *via* their reaction with lysine residues, has been reported.²⁸ Further investigations into the mechanism of action of **12a** were not conducted. Some aminothiazoles have recently been identified as frequent hitters from a fragment screening set and dubbed promiscuous 2-aminothiazoles (PrATs).²⁹ The reason for the discrepancy between the activity of the HTS sample and the resynthesized material is not clear. Numerous mechanisms for false positives in HTS are possible, including the presence of trace impurities or protein aggregation, and further effort was not expended eliminating these possibilities.³⁰

Three HTS hits in the nicotinonitrile series (**4a**, **19**, and **31**) were synthesised and reassayed (Tables 3 and 4). The results for the glycine derivative **4a** and proline methyl ester derivative **19** were in good agreement with the HTS IC₅₀ values. In contrast, the propan-2-one derivative **31** was 50-fold less active than the HTS result. On this basis, a limited series of compounds was prepared to establish preliminary SARs and to determine the minimum inhibitory pharmacophore. The SARs for the 4- and 6-substitutents were delineated keeping the 2-thio substituent as the glycine amide (Table 3). The 4,6-diphenyl, 4-phenyl-6-methyl and 4,6-dimethyl compounds (**4d**, **4j** and **4k**, respectively) were each devoid of activity. The 4-(2-fluorophenyl) derivative **4c** was 7-fold less active than the 4-(4-fluorophenyl) derivative **4a**, whereas the 4-(3-fluorophenyl) derivative **4b** lacked measurable potency. The combination of 2-fluoro and 4-fluoro substituents (**4f**) was not additive and resulted in a 15-fold loss of potency compared with **4a**. The 4-(4-pyridyl) derivative **4g** exhibited a 13-fold loss in potency compared to **4a**, despite the similar electronic properties of the rings. Substitution of the 4-phenyl group with 4-trifluoromethyl **4e**, or 4-methoxy **4h** resulted in loss of activity.

The SARs for the thioether side-chain were investigated (Table 4). The pyridine thiol **14a** lacking the amide side-chain showed a 20-fold loss in potency compared to **4a**. The glycine ethyl ester **15l** showed similar activity to the proline methyl ester derivative **19**, and was 4-fold less potent than the corresponding glycine derivative **4a**. In contrast, the glycine amide **17** lacked measurable activity. The shorter, unsubstituted amide **20** showed weak activity, whereas the corresponding ester **21** was inactive. Two thioalkyl carboxylic acids **23a** and **23b** were inactive, as was the corresponding amine **28**, demonstrating the requirement for the amide group in the sidechain for potency. Comparison of the 4-fluorophenyl propan-2-one derivative **31** with the 4-pyridyl derivative **32** showed a 5-fold loss in potency consistent with the results in the glycine amide series (**4a** and **4g**).

Overall, each of the changes made to the hit compounds in the nicotinonitrile series (**4a**, **19**, and **31**) resulted in loss of potency. Modifications to the aromatic and side-chain substituents revealed a highly constrained pharmacophore and limited SAR. As a result, no further optimisation of this series was attempted. Interestingly, 3-cyano-4,6-diphenyl-pyridines have been identified recently as inhibitors of the PA-PB1 protein-protein interaction for influenza.³¹

The cyanopyrimidines **5a-c** showed reasonable activity against ERK5, with IC₅₀ values in the 12-88 µM range (Table 5), and generally consistent with the HTS values. The activity against ERK5 in this series was promising, but the series had also been selected for development against another target internally. For this reason, no further analogues were prepared. Kinase inhibitors incorporating a 5-cyanopyrimidine core have been reported, e.g. Wee1 inhibitors³², and CDK2 inhibitors³³.

Five 4-benzoylpyrrole-2-carboxamides (**6a-e**) gave good potency in the HTS. Upon resynthesis and retesting, the 2,3-dichlorobenzoyl-*N*-(4-fluorobenzyl) substituted analogue **6a** maintained significant activity (IC₅₀ = 3.7 µM) despite a 5-fold loss in potency compared to the HTS result (Table 6). Similarly, the 2-trifluoromethylbenzoyl-*N*-methyl substituted analogue **6d** gave a two-fold drop in activity (IC₅₀ = 9.6 µM) compared to the HTS result, and the benzoyl-*N*-methyl-3-pyridyl derivative **6e** gave a 3-fold drop in activity (IC₅₀ = 26 µM). In contrast, the resynthesized 2,4-dichlorobenzoyl analogues **6b** and **6c** bearing either the *N,N*-dimethylamide or *N*-phenethylamide substituents, respectively, showed no activity.

Encouraged by these results, a small series of aroylpyrroles was prepared. Compounds were designed to establish the minimum kinase binding pharmacophore, and to explore possibilities to gain potency and selectivity by variation of the amide substituent. The benzoyl substituent was fixed as most potent 2,3-dichlorophenyl for all these examples.

Series (**6f-n**) was prepared to explore simple variations to the amide moiety (Table 7). Monomethyl amide **6f** was equipotent with the parent 4-fluorobenzyl amide **6a**, whereas the dimethyl amide **6g** was 7-fold less potent. Introduction of the 3-pyridylmethyl amide from **6e** or the 4-pyridylmethyl amide **6h**, retained potency, whereas the benzyl derivative **6k** and 2-pyridyl derivative **6j** were less potent, and phenylethyl amide **6l** was inactive. Similar to **6g**, *N*-methyl-(3-pyridylmethyl) amide derivative **6n** was 7-fold less potent than primary amide **6i**. Importantly,

1 methylation of the pyrrole NH (**6m**) completely abolished ERK5 activity, indicating an essential interaction with the
2 kinase at this position. In contrast, the relatively small drop in activity for the secondary amides **6g** and **6n** suggested
3 the amide NH was not forming a critical interaction, and that the drop in potency could be related to the
4 conformational preference of the amide group. With this in mind, a limited number of conformationally restricted, 5-
5 and 6-membered cyclic secondary amides were investigated (Table 8). The 3,4-dihydro-2,6-naphthyridinyl and
6 isoindolinyl derivatives (**6o** and **6q**) were inactive. In contrast, 3,4-dihydroisoquinolinyl **6p** was 5-fold less potent than
7 **6h**, a comparable to the loss in potency seen for the *N*-methyl analogues, whereas the pyrrolidinopyridinyl **6r** was
8 equipotent with **6h**. Selected examples in this series were assayed in an orthogonal LANCE™ assay format (see
9 supporting information), based on time-resolved fluorescence resonance energy transfer (FRET), to eliminate the
10 possibility of false positives. In all cases, the LANCE results were comparable with those obtained using the IMAP
11 assay.
12

13 In order to establish the minimum kinase binding pharmacophore, systematic isosteric replacements to the amide
14 group were made. The acetyl derivative **39** and the 1,3-diketone **44** were inactive (Table 9). In contrast, the
15 unsaturated ketone **40** and the cyclopropyl ketone **42** retained similar activity to the parent **6a**, whereas the
16 saturated ketone **41** was 10-fold less active. These results confirm that the amide NH is not required for activity, and
17 that conformational rigidity at this position is favourable. The loss of activity for diketone **44** was explained by the
18 preferred enol tautomer lacking an essential H-bond to the kinase via the ketone adjacent to the pyrrole.
19

20 The most potent pyrrole inhibitor **6h** was submitted for a kinase selectivity screen and gave a promising selectivity
21 profile. Of the 20 kinases, screened only one kinase (SAPK2a or p38α MAP kinase) was inhibited at >50% inhibition
22 (10 μM). Subsequent to our identification of pyrrole-2-carboxamides as ERK5 inhibitors, similar compounds, e.g. **45**,
23 have been independently identified as p38α MAP kinase inhibitors with micromolar activity.³⁴ The X-ray structure of
24 **45** shows it bound to the hinge of the kinase via hydrogen bonds from the pyrrole NH and the carboxamide carbonyl,
25 with the aryl portion occupying the lipophilic region close to the gatekeeper, and the furan binding in the outer
26 lipophilic region. ERK5 shares 48% sequence homology with p38α MAP kinase, and 58% homology in the kinase
27 domain. In addition, the gatekeeper residues of the kinases are similar, with leucine in ERK5 and threonine in p38α
28 MAP kinase. The ERK5 SAR for our series is consistent with a similar binding mode to ERK5 as seen in the p38 X-ray
29 structure, in particular the donor/acceptor doublet of H-bonds from the pyrrole NH and amide carbonyl to the
30 kinase.
31

32 At this point, given the similarity between the published p38α MAP kinase inhibitors and our hit series, we needed
33 to establish selectivity vs p38α MAP kinase to provide useful ERK5 tool compounds or therapeutic agents.³⁴⁻³⁵ Thus,
34 selected compounds were counterscreened against p38α MAP kinase using a LANCE assay. As anticipated, the 2-
35 pyridyl derivatives **6j** and 3,4-dihydroisoquinolinyl derivative **6p** were equipotent for both p38α MAP kinase and
36 ERK5. Importantly, the pyrrolidinopyridinyl derivative **6r** was inactive in the p38α assay. The ability to eliminate p38α
37 MAP kinase activity whilst maintaining ERK5 activity by variation of the amide side chain was not readily predicted
38
39
40
41
42
43
44
45
46
47
48
49
50
51
52
53
54
55
56
57
58
59
60

from the published p38 α X-ray structure and points to differing structural requirements around the amide side-chain that may be exploited in further development of the series.

CONCLUSIONS

The IMAP FP high-throughput screen for ERK5 returned four distinct chemical series as hits. Synthesis of the hits and selected close analogues demonstrated that the HTS activity of the benzothiazoles **3** was not reproducible, activity for the cyanopyridine hits (**4a**, **19**) was reproducible, but the limited scope to develop the SAR ruled this series out, and two series with confirmed active hits. The lack of activity of these hits was disappointing but not atypical in screening campaigns. The cyanopyrimidine hits **5a-c** were not pursued for reasons of competition. The remaining series, the pyrrole carboxamides **6a-e**, demonstrated consistent ERK5 activity, with SARs consistent with a kinase hinge binder. Selectivity against the close homologue p38 α MAP kinase was achieved without loss of ERK5 activity through minor structural modification, and a representative example **6h** showed an acceptable kinase selectivity profile in a panel. At this stage the pyrrole carboxamides demonstrated tractable synthesis, intelligible preliminary SARs, and promising selectivity. The relatively modest kinase inhibitory activity achieved at this stage did not give any concern as the pharmacophore established presented opportunities to optimise potency at both the benzoyl and amide portions, independently. Having demonstrated the necessary requirements to progress to the hit-to-lead optimisation stage, further SAR studies were undertaken, with an initial focus on improving potency, which will be reported separately.³⁶

EXPERIMENTAL SECTION

IMAP Substrate mapping

Non-phosphorylated and phosphorylated versions of each ERK5 sequence (Table 1) were obtained from the CRUK Peptide Synthesis Research Services group. The substrate finder kit was used according to the manufacturer's instructions. Reaction buffer (10 μ L) containing ATP (100 μ M) was added to wells of the plate to reconstitute 5-FAM labeled substrates. Reaction buffer (10 μ L) with or without ERK5 (6.4 ng/ μ L) was added to appropriate wells of the plate, to generate background controls and positive controls. The reaction was incubated for 1 hour at ambient temperature after which IMAP Binding Solution (60 μ L) was added. After a further 1 hour of incubation the fluorescence polarisation was measured. The results were analysed using the IMAP Substrate Mapper provided with the kit.

Kinetic characterisation of ERK5

Reactions were carried out with varying concentrations of ATP at constant substrate and enzyme concentrations. Due to limitations of the IMAP FP assay with respect to ATP concentrations, we utilised a transfer method to increase the maximum concentration of ATP that can be used. Reactions were conducted as normal in 10 μ L reaction volume. After either 1, 2, 3 or 4 hour incubation period at 37°C, 4 μ L of the reaction was transferred to 196 μ L of reaction buffer followed by a subsequent transfer of 10 μ L of this solution to 30 μ L of IMAP Binding Solution. Rates

of reaction at 1 hour reaction time at the range of substrate concentrations were determined, and kinetic parameters were determined by non-linear regression fitting of the data to the Michaelis-Menten equation (Equation 1) ; curve fitting was performed using GraphPad Prism software.³⁷

ERK5 High-throughput Screen

Compounds were assayed in a 10 μ L reaction mixture per well containing: 1 in 700 dilution of ERK5 stock from CRT, 100 nM peptide R7129 and 100 μ M of ATP. The reactions were performed with 10 mM Tris-HCl (pH 7.2), 10 mM $MgCl_2$, 0.05% NaN_3 and 0.01% Tween-20. Reactions were incubated for 3 hours at 37°C, followed by addition of 30 μ L of IMAP binding solution (1 in 600 dilution of IMAP binding reagent in 60% Binding Buffer A and 40% Binding Buffer B) and a further incubation for 2 hours at ambient temperature. Plates were read on an Analyst HT microplate reader and the data analysed using ActivityBase.

ERK5 IC₅₀ Determination (IMAP)

The enzyme reaction was run as described for the HTS but using 300 μ M ATP, 250 nM peptide and a reduced incubation time of 2 hours at 37°C. 1 μ L of this reaction was then transferred to a new assay plate and 9 μ L of reaction buffer was added followed by 30 μ L of IMAP binding solution.

X-ray crystallography

Data were collected on an Oxford Diffraction Gemini A Ultra diffractometer for **3i**, using MoK α radiation (λ = 0.71073 Å) at 150K, and on a Bruker Apex2 diffractometer for **3a** and **12a**, using synchrotron radiation (λ = 0.6946 Å; SRS station 9.8, Daresbury Laboratory) at 120 K because of the very small size of crystals available. Corrections were made for synchrotron beam decay and for absorption and other systematic effects on the basis of repeated and equivalent data. The structures were solved by direct methods and refined on all unique F^2 values with anisotropic non-hydrogen atoms, with freely refined isotropic H atoms bonded to N, and with a riding model for H atoms bonded to C. All four structures are fully ordered; **3i** have two independent molecules in the asymmetric unit, and the non-centrosymmetric but achiral crystal structure of **3i** displays inversion twinning with essentially equal components. Full crystallographic details are given in the Supporting information. Programs were standard Oxford Diffraction CrysAlisPro³⁸ and Bruker Apex2³⁹ for data collection and processing, and SHELXTL⁴⁰ and SHELXL-2014_ENREF_52_ENREF_53⁴¹ for structure solution and refinement. CCDC references: 1410001, 141003, and 1410004.

ASSOCIATED CONTENT

Supporting Information

Additional screening and synthesis information, X-ray crystal structure data for compounds **12a**, **3a**, and **3i**, synthetic procedures, ERK5 and p38 α LANCE assay protocols, kinase selectivity data for **6h**.

AUTHOR INFORMATION

Corresponding Author

*E-mail: Ian.Hardcastle@ncl.ac.uk

Funding

This work was supported by Cancer Research UK (C240/A7409, C1296/A6963 and C2115/A21421), EPSRC equipment grant (EP/F03637X/1), and the synchrotron component of the UK National Crystallography Service 2001–2010 (EP/D07746X/1).

Notes

The authors declare no competing financial interests.

ACKNOWLEDGEMENTS

We thank CCLRC for access to synchrotron diffraction facilities at SRS. The use of the EPSRC National Mass Spectroscopy Facility, Swansea University is gratefully acknowledged.

REFERENCES

1. (a) Zhou, G.; Bao, Z. Q.; Dixon, J. E., Components of a New Human Protein Kinase Signal Transduction Pathway. *J. Biol. Chem.* **1995**, *270* (21), 12665-12669; (b) Zhou, G. C.; Bao, A.; Guan, K. L.; Dixon, J. E., Specific Interactions Between Newly Identified Human Kinases, Mek5 And Erk5. *FASEB J.* **1995**, *9* (6), A1306-A1306; (c) Abe, J.; Kusuvara, M.; Ulevitch, R. J.; Berk, B. C.; Lee, J. D., Big mitogen-activated protein kinase 1 (BMK1) is a redox-sensitive kinase. *J. Biol. Chem.* **1996**, *271* (28), 16586-16590.
2. Hayashi, M.; Lee, J. D., Role of the BMK1/ERK5 signaling pathway: lessons from knockout mice. *J. Mol. Med.* **2004**, *82* (12), 800-8.
3. English, J. M.; Pearson, G.; Hockenberry, T.; Shivakumar, L.; White, M. A.; Cobb, M. H., Contribution of the ERK5/MEK5 pathway to Ras/Raf signaling and growth control. *J. Biol. Chem.* **1999**, *274* (44), 31588-92.
4. Wang, X.; Tournier, C., Regulation of cellular functions by the ERK5 signalling pathway. *Cell Signal* **2006**, *18* (6), 753-60.
5. Roberts, O. L.; Holmes, K.; Muller, J.; Cross, D. A.; Cross, M. J., ERK5 and the regulation of endothelial cell function. *Biochem. Soc. Trans.* **2009**, *37* (Pt 6), 1254-9.
6. (a) Kato, Y.; Kravchenko, V. V.; Tapping, R. I.; Han, J.; Ulevitch, R. J.; Lee, J.-D., BMK1/ERK5 regulates serum-induced early gene expression through transcription factor MEF2C. *EMBO J* **1997**, *16* (23), 7054-7066; (b) Yang, C. C.; Ornatsky, O. I.; McDermott, J. C.; Cruz, T. F.; Prody, C. A., Interaction of myocyte enhancer factor 2 (MEF2) with a mitogen-activated protein kinase, ERK5/BMK1. *Nucleic Acids Res* **1998**, *26* (20), 4771-4777; (c) Kato, Y.; Tapping, R. I.; Huang, S.; Watson, M. H.; Ulevitch, R. J.; Lee, J.-D., Bmk1/Erk5 is required for cell proliferation induced by epidermal growth factor. *Nature* **1998**, *395* (6703), 713-716; (d) English, J. M.; Pearson, G.; Baer, R.;

- Cobb, M. H., Identification of Substrates and Regulators of the Mitogen-activated Protein Kinase ERK5 Using Chimeric Protein Kinases. *J. Biol. Chem.* **1998**, *273* (7), 3854-3860; (e) Kamakura, S.; Moriguchi, T.; Nishida, E., Activation of the Protein Kinase ERK5/BMK1 by Receptor Tyrosine Kinases. *J. Biol. Chem.* **1999**, *274* (37), 26563-26571; (f) Pearson, G.; English, J. M.; White, M. A.; Cobb, M. H., ERK5 and ERK2 Cooperate to Regulate NF- κ B and Cell Transformation. *J. Biol. Chem.* **2001**, *276* (11), 7927-7931; (g) Terasawa, K.; Okazaki, K.; Nishida, E., Regulation of c-Fos and Fra-1 by the MEK5-ERK5 pathway. *Genes Cells* **2003**, *8* (3), 263-273.
7. (a) Hayashi, M.; Fearn, C.; Eliceiri, B.; Yang, Y.; Lee, J. D., Big mitogen-activated protein kinase 1/extracellular signal-regulated kinase 5 signaling pathway is essential for tumor-associated angiogenesis. *Cancer Res.* **2005**, *65* (17), 7699-7706; (b) Nhat-Tu, L.; Heo, K.-S.; Takei, Y.; Lee, H.; Woo, C.-H.; Chang, E.; McClain, C.; Hurley, C.; Wang, X.; Li, F.; Xu, H.; Morrell, C.; Sullivan, M. A.; Cohen, M. S.; Serafimova, I. M.; Taunton, J.; Fujiwara, K.; Abe, J.-I., A Crucial Role for p90RSK-Mediated Reduction of ERK5 Transcriptional Activity in Endothelial Dysfunction and Atherosclerosis. *Circulation* **2013**, *127* (4), 486-+; (c) Ranganathan, A.; Pearson, G. W.; Chrestensen, C. A.; Sturgill, T. W.; Cobb, M. H., The MAP kinase ERK5 binds to and phosphorylates p90 RSK. *Arch. Biochem. Biophys.* **2006**, *449* (1-2), 8-16.
 8. (a) Drew, B. A.; Burow, M. E.; Beckman, B. S., MEK5/ERK5 pathway: the first fifteen years. *Biochim Biophys Acta* **2012**, *1825* (1), 37-48; (b) Lochhead, P. A.; Gilley, R.; Cook, S. J., ERK5 and its role in tumour development. *Biochem. Soc. Trans.* **2012**, *40* (1), 251-6.
 9. (a) Mehta, P. B.; Jenkins, B. L.; McCarthy, L.; Thilak, L.; Robson, C. N.; Neal, D. E.; Leung, H. Y., MEK5 overexpression is associated with metastatic prostate cancer, and stimulates proliferation, MMP-9 expression and invasion. *Oncogene* **2003**, *22* (9), 1381-1389; (b) McCracken, S. R.; Ramsay, A.; Heer, R.; Mathers, M. E.; Jenkins, B. L.; Edwards, J.; Robson, C. N.; Marquez, R.; Cohen, P.; Leung, H. Y., Aberrant expression of extracellular signal-regulated kinase 5 in human prostate cancer. *Oncogene* **2008**, *27* (21), 2978-88.
 10. Montero, J. C. O., A; Abad, M; Ortiz-Ruiz, M, J; Pandiella, A; Esparis-Ogando, A, Expression of ERK5 in Early Stage Breast Cancer and Association with Disease Free Survival Identifies this Kinase as a Potential Therapeutic Target. *PLoS ONE* **2009**, *4* (5), 5565.
 11. Zen, K.; Yasui, K.; Nakajima, T.; Zen, Y.; Zen, K.; Gen, Y.; Mitsuyoshi, H.; Minami, M.; Mitsufuji, S.; Tanaka, S.; Itoh, Y.; Nakanuma, Y.; Taniwaki, M.; Arii, S.; Okanoue, T.; Yoshikawa, T., ERK5 is a target for gene amplification at 17p11 and promotes cell growth in hepatocellular carcinoma by regulating mitotic entry. *Genes Chrom. Cancer* **2009**, *48* (2), 109-120.
 12. Arias-González, L.; Moreno-Gimeno, I.; del Campo, A. R.; Serrano-Oviedo, L.; Valero, M. L.; Esparís-Ogando, A.; de la Cruz-Morcillo, M. Á.; Melgar-Rojas, P.; García-Cano, J.; Cimas, F. J.; Hidalgo, M. J. R.; Prado, A.; Callejas-Valera, J. L.; Nam-Cha, S. H.; Giménez-Bachs, J. M.; Salinas-Sánchez, A. S.; Pandiella, A.; del Peso, L.; Sánchez-Prieto, R., ERK5/BMK1 Is a Novel Target of the Tumor Suppressor VHL: Implication in Clear Cell Renal Carcinoma. *Neoplasia* **2013**, *15* (6), 649-659.
 13. Tatake, R. J.; O'Neill, M. M.; Kennedy, C. A.; Wayne, A. L.; Jakes, S.; Wu, D.; Kugler Jr, S. Z.; Kashem, M. A.; Kaplita, P.; Snow, R. J., Identification of pharmacological inhibitors of the MEK5/ERK5 pathway. *Biochem. Biophys. Res. Commun.* **2008**, *377* (1), 120-125.

14. Yang, Q.; Deng, X.; Lu, B.; Cameron, M.; Fearn, C.; Patricelli, M. P.; Yates, J. R.; Gray, N. S.; Lee, J.-D., Pharmacological Inhibition of BMK1 Suppresses Tumor Growth through Promyelocytic Leukemia Protein. *Cancer Cell* **2010**, *18* (4), 396.
15. Elkins, J. M.; Wang, J.; Deng, X.; Pattison, M. J.; Arthur, J. S. C.; Erazo, T.; Gomez, N.; Lizcano, J. M.; Gray, N. S.; Knapp, S., X-ray Crystal Structure of ERK5 (MAPK7) in Complex with a Specific Inhibitor. *J. Med. Chem.* **2013**, *56* (11), 4413-4421.
16. Sureban, S. M.; May, R.; Weygant, N.; Qu, D.; Chandrasekaran, P.; Bannerman-Menson, E.; Ali, N.; Pantazis, P.; Westphalen, C. B.; Wang, T. C.; Houchen, C. W., XMD8-92 inhibits pancreatic tumor xenograft growth via a DCLK1-dependent mechanism. *Cancer Lett* **2014**, *351* (1), 151-161.
17. Rovida, E.; Di Maira, G.; Tusa, I.; Cannito, S.; Paternostro, C.; Navari, N.; Vivoli, E.; Deng, X.; Gray, N. S.; Esparís-Ogando, A.; David, E.; Pandiella, A.; Dello Sbarba, P.; Parola, M.; Marra, F., The mitogen-activated protein kinase ERK5 regulates the development and growth of hepatocellular carcinoma. *Gut* **2015** *64* (9), 1454-1465.
18. Finegan, K. G.; Perez-Madrigal, D.; Hitchin, J. R.; Davies, C. C.; Jordan, A. M.; Tournier, C., ERK5 Is a Critical Mediator of Inflammation-Driven Cancer. *Cancer Res.* **2015**, *75* (4), 742-753.
19. (a) Collins, I.; Workman, P., New approaches to molecular cancer therapeutics. *Nat Chem Biol* **2006**, *2* (12), 689-700; (b) Hughes, J. P.; Rees, S.; Kalindjian, S. B.; Philpott, K. L., Principles of early drug discovery. *British Journal of Pharmacology* **2011**, *162* (6), 1239-1249.
20. (a) Barton, D.; Ollis, W. D., *Heterocyclic Compounds*. Pergamon: Oxford, New York, 1979; Vol. 4; (b) Jordan, A. D.; Luo, C.; Reitz, A. B., Efficient Conversion of Substituted Aryl Thioureas to 2-Aminobenzothiazoles Using Benzyltrimethylammonium Tribromide. *J. Org. Chem.* **2003**, *68* (22), 8693-8696; (c) Ding, Q.; He, X.; Wu, J., Synthesis of 2-Aminobenzothiazole via Copper(I)-Catalyzed Tandem Reaction of 2-Iodobenzenamine with Isothiocyanate. *J. Comb. Chem.* **2009**, *11* (4), 587-591; (d) Li, Z.; Xiao, S.; Tian, G.; Zhu, A.; Feng, X.; Liu, J., Microwave Promoted Environmentally Benign Synthesis of 2-Aminobenzothiazoles and Their Urea Derivatives. *Phosphorus Sulfur Silicon Relat. Elem.* **2008**, *183* (5), 1124-1133; (e) Jordan, A. D.; Luo, C.; Reitz, A. B., Efficient Conversion of Substituted Aryl Thioureas to 2-Aminobenzothiazoles Using Benzyltrimethylammonium Tribromide. *J. Org. Chem.* **2003**, *68* (22), 8693-8696.
21. Nagarajan, S. R.; De Crescenzo, G. A.; Getman, D. P.; Lu, H.-F.; Sikorski, J. A.; Walker, J. L.; McDonald, J. J.; Houseman, K. A.; Kocan, G. P.; Kishore, N.; Mehta, P. P.; Funkes-Shippy, C. L.; Blystone, L., Discovery of novel benzothiazolesulfonamides as potent inhibitors of HIV-1 protease. *Bioorg. Med. Chem.* **2003**, *11* (22), 4769-4777.
22. Shestopalov, A. M.; Nikishin, K. G., One stage synthesis of 4,6-diaryl-3-cyanopyridine-2(1H)-thiones. *Chem. Heterocycl. Compd.* **1998**, *34*, 1093.
23. Hepworth, J. D., Aminoacetone Semicarbazone Hydrochloride. *Organic Syntheses, Coll. Vol.* **1973**, *5*, 27.
24. Schmidt, H.-W.; Koitz, G.; Junek, H., A convenient synthesis of 2-substituted 4-amino-5-pyrimidinecarbonitriles. *J. Heterocycl. Chem.* **1987**, *24* (5), 1305-1307.
25. Ranu, B. C.; Dutta, J.; Guchhait, S. K., Indium metal as a reducing agent. Selective reduction of the carbon-carbon double bond in highly activated conjugated alkenes. *Org. Lett.* **2001**, *3* (16), 2603-2605.

- 1
2
3
4
5
6
7
8
9
10
11
12
13
14
15
16
17
18
19
20
21
22
23
24
25
26
27
28
29
30
31
32
33
34
35
36
37
38
39
40
41
42
43
44
45
46
47
48
49
50
51
52
53
54
55
56
57
58
59
60
26. Corey, E. J.; Chaykovsky, M., Dimethyloxosulfonium methylide ((CH₃)₂SOCH₂) and dimethylsulfonium methylide ((CH₃)₂SCH₂). Formation and application to organic synthesis. *J. Am. Chem. Soc.* **1965**, *87* (6), 1353-1364.
27. Ciaccio, J. A.; Aman, C. E., "Instant Methylide" Modification of the Corey–Chaykovsky Cyclopropanation Reaction. *Synth. Commun.* **2006**, *36* (10), 1333-1341.
28. Wu, Q.; Caine, J. M.; Thomson, S. A.; Slavica, M.; Grunewald, G. L.; McLeish, M. J., Time-dependent inactivation of human phenylethanolamine N-methyltransferase by 7-isothiocyanatotetrahydroisoquinoline. *Bioorg. Med. Chem. Lett.* **2009**, *19* (4), 1071-1074.
29. Devine, S. M.; Mulcair, M. D.; Debono, C. O.; Leung, E. W. W.; Nissink, J. W. M.; Lim, S. S.; Chandrashekar, I. R.; Vazirani, M.; Mohanty, B.; Simpson, J. S.; Baell, J. B.; Scammells, P. J.; Norton, R. S.; Scanlon, M. J., Promiscuous 2-Aminothiazoles (PrATs): A Frequent Hitting Scaffold. *J. Med. Chem.* **2015**, *58* (3), 1205-1214.
30. Baell, J. B.; Holloway, G. A., New Substructure Filters for Removal of Pan Assay Interference Compounds (PAINS) from Screening Libraries and for Their Exclusion in Bioassays. *J. Med. Chem.* **2010**, *53* (7), 2719-2740.
31. Trist, I. M. L.; Nannetti, G.; Tintori, C.; Fallacara, A. L.; Deodato, D.; Mercorelli, B.; Palù, G.; Wijtmans, M.; Gospodova, T.; Edink, E.; Verheij, M.; de Esch, I.; Viteva, L.; Loregian, A.; Botta, M., 4,6-Diphenylpyridines as Promising Novel Anti-Influenza Agents Targeting the PA–PB1 Protein–Protein Interaction: Structure–Activity Relationships Exploration with the Aid of Molecular Modeling. *J. Med. Chem.* **2016**, *59* (6), 2688-2703.
32. Thomas, A. P. Preparation and formulation of 4-amino-5-cyano-2-anilino-pyrimidines as inhibitors of cell-cycle kinases for pharmaceutical use in the treatment of cancer. 2001.
33. Marchetti, F.; Cano, C.; Curtin, N. J.; Golding, B. T.; Griffin, R. J.; Haggerty, K.; Newell, D. R.; Parsons, R. J.; Payne, S. L.; Wang, L. Z.; Hardcastle, I. R., Synthesis and biological evaluation of 5-substituted O4-alkylpyrimidines as CDK2 inhibitors. *Org. Biomol. Chem.* **2010**, *8* (10), 2397-2407.
34. Down, K.; Bamborough, P.; Alder, C.; Campbell, A.; Christopher, J. A.; Gerelle, M.; Ludbrook, S.; Mallett, D.; Mellor, G.; Miller, D. D.; Pearson, R.; Ray, K.; Solanke, Y.; Somers, D., The discovery and initial optimisation of pyrrole-2-carboxamides as inhibitors of p38[alpha] MAP kinase. *Bioorg. Med. Chem. Lett.* **2010**, *20* (13), 3936-3940.
35. Workman, P.; Collins, I., Probing the Probes: Fitness Factors For Small Molecule Tools. *Chem. Biol.* **2010**, *17* (6), 561-577.
36. Reuillon, T.; Miller, D.; Myers, S.; Molyneux, L.; Cano, C.; Hardcastle, I. R.; Griffin, R. J.; Rigoreau, L.; Golding, B. T.; Noble, M. E. N. Pyrrolcarboxamide Derivatives For The Inhibition of ERK5. WO/2016/042341.
37. *Prism*, 6; GraphPad Software Inc: 2014.
38. *CrysAlisPro*, Oxford Diffraction: Oxford, UK, 2008.
39. *Apex2*, Bruker AXS inc.: Madison, MI, USA, 2008.
40. Sheldrick, G., A short history of SHELX. *Acta Crystallogr., Sect. A* **2008**, *64* (1), 112-122.
41. Sheldrick, G., Crystal structure refinement with SHELXL. *Acta Crystallogr., Sect. C* **2015**, *71* (1), 3-8.

1

2

3

4

5

6

7

8

9

10

11

12

13

14

15

16

17

18

19

20

21

22

23

24

25

26

27

28

29

30

31

32

33

34

35

36

37

38

39

40

41

42

43

44

45

46

47

48

49

50

51

52

53

54

55

56

57

58

59

60

EQUATIONS

Equation 1

$$\frac{v}{[E]} = \frac{k_{cat}[S]}{(K_m + [S])}$$

Equation 2

$$Z' = 1 - \frac{3\sigma_{c+} + 3\sigma_{c-}}{|\mu_{c+} - \mu_{c-}|}$$

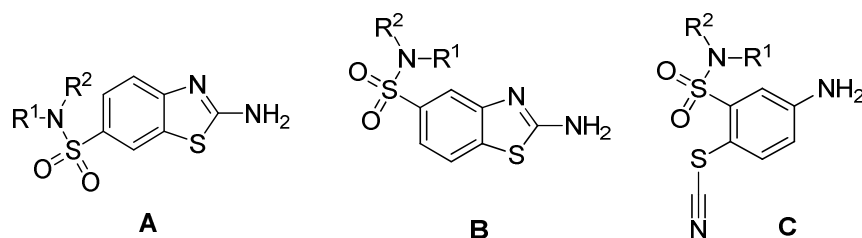
Where σ and μ represent the standard deviation and mean of the positive (c+) and negative (c-) plate controls, respectively.

TABLES

Table 1

Number	Sequence
166	5-FAM-AGRSPVD
168	5-FAM-EAGRSPVDS
170	5-FAM-HEAGRSPVDSL
172	5-FAM-RHEAGRSPVDSL
174	5-FAM-TRHEAGRSPVDSLSS

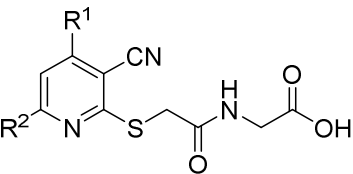
Table 2



Compound	Structure	R ¹	R ²	ERK5 IC ₅₀ (μM)	
				HTS	Resynthesized ^a
3a	A	-(CH ₂) ₄ -		0.057	51 ± 5.0
3b	A	Et	Me	0.087	85 ± 5.0
3c	A	Me	H	0.087	-
3d	A	Et	H	0.11	-
3e	A	CH ₂ =CHCH ₂ -	H	0.13	-
3f	A	<i>s</i> -Bu	H	0.13	-
3g	A	-(CH ₂) ₅ -		0.46	-
3h	A	<i>i</i> -Pr	H	0.60	-
3i	A	<i>n</i> -Pr	H	0.89	>120 ^b
3j	A	Et	Et	0.93	-
3k	A	-(CH ₂) ₂ O(CH ₂) ₂ -		5.13	-
9a	B	-(CH ₂) ₄ -		-	29 ± 1.3
9b	B	Et	Me	-	21 ± 1.5
12a	C	-(CH ₂) ₄ -		-	2.3 ± 1.5
12b	C	Et	Me	-	>120 ^b

a) Values are the mean of at least 3 determinations ± SD; b) n = 2

Table 3: ERK5 inhibitory activity of nicotinonitrile series **4a-k**.



Compd	R ¹	R ²	ERK5 IC ₅₀ (μM)	
			HTS	Resynthesized ^a
4a	4-F-Ph	Ph	1.6	4.9 ± 0.3
4b	3-F-Ph	Ph	-	>120 ^b
4c	2-F-Ph	Ph	-	34.3 ± 6.4
4d	Ph	Ph	-	>120 ^b
4e	4-(CF ₃)-Ph	Ph	-	>120 ^b
4f	2,4-di-F-Ph	Ph	-	72.9 ± 26.1
4g	4-Py	Ph	-	65.1 ± 12.4
4h	4-MeOPh	Ph	-	>120 ^b
4i	Ph	4-MeOPh	-	>120 ^b
4j	Ph	CH ₃	-	>120 ^b
4k	CH ₃	CH ₃	-	>120 ^b

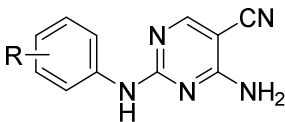
a) Values are the mean of at least 3 determinations ± SD; b) n = 2

Table 4: ERK5 inhibitory activity of nicotinonitrile series **14a,15l, 17,19-21, 23, 28** and **31-32**.

Compound	R	R ¹	R ²	ERK5 IC ₅₀ (μM)	
				HTS	Resynthesized ^a
14a	H	Ph	4-F-Ph	-	111 ± 6.5
15l		Ph	4-F-Ph	-	20.9 ± 1.6 ^c
17		Ph	4-F-Ph	-	>120
19		Ph	4-F-Ph	31	29.4 ± 3.7 ^c
20		Ph	4-F-Ph	-	117 ± 18
21		Ph	4-F-Ph	-	>120
23a		Ph	4-F-Ph	-	>120 ^d
23b		Ph	4-F-Ph	-	>120 ^d
28		Ph	4-F-Ph	-	>120
31		Ph	4-F-Ph	0.4	20.5 ± 1.3
32		Ph	4-Py	-	104.9 ± 6.5

a) Values are the mean of at least 3 determinations ± SD b) n = 1; c) n = 2; d) precipitation observed at 1.2 mM in 40% DMSO;

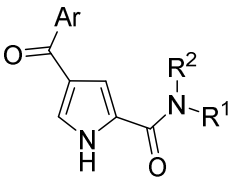
Table 5: ERK5 inhibitory activity of pyrimidine series **5a-c**.



Compound	R	ERK5 IC ₅₀ (μM)	
		HTS	Resynthesized ^a
5a	2-CH ₃	26	88 ± 3
5b	3-OCH ₃	11	23 ± 7
5c	4-F	6.5	12 ± 3

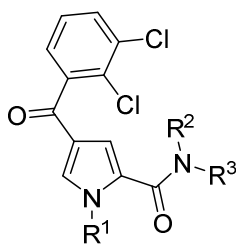
a) Values are the mean of at least 3 determinations ± SD

Table 6 : ERK5 inhibitory activity of pyrrole carboxamides (**6a-e**)



Compound	Ar	R ¹	R ²	ERK5 IC ₅₀ (μM)	
				HTS	Resynthesized ^a
6a			H	0.66	3.7
6b		CH ₃	CH ₃	1.89	>120 ^b
6c			H	3.50	>120 ^b
6d		CH ₃	H	4.32	9.6 ± 3.9
6e			H	8.0	26.0 ± 1.2

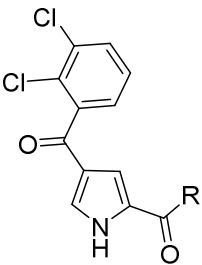
a) Values are the mean of at least 3 determinations ± SD; b) n = 2

Table 7. ERK5 SAR for pyrrole carboxamides (**6f-n**)

Compound	R ¹	R ²	R ³	ERK5 IC ₅₀ (μM)	
				IMAP ^a	LANCE ^a
6f	H	H	CH ₃	3.3 ± 1.0 ^b	3.6 ± 1.0
6g	H	CH ₃	CH ₃	24 ± 27 ^c	44 ± 24
6h	H	H		2.0 ± 2.0 ^d	-
6i	H	H		3.8 ± 3.7 ^c	1.1 ± 0.4 ^c
6j	H	H		7.2 ± 0.02	3.9 ± 0.8
6k	H	H		21 ^e	-
6l	H	H		>120	-
6m	CH ₃	H		>120	-
6n	H	CH ₃		25 ± 1.3	13 ± 1.9

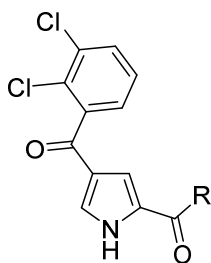
a) determinations ± standard deviation (mean of n = 2 unless otherwise stated); b) IC₅₀ mean of n = 4; c) IC₅₀ mean of n = 6; d) IC₅₀ mean of n = 10; e) IC₅₀ n = 1.

Table 8. SAR for cyclic pyrrole carboxamides (**6j**, **6o-r**) against ERK5 and p38α.



Compound ID	R	ERK5 IC ₅₀ (μM) ^a		p38α LANCE
		IMAP	LANCE	IC ₅₀ (μM) ^a
6j		7.2 ± 0.03		4.3 ± 1.2 ^b
6o		>120	-	
6p		11 ± 2.3 ^b	25 ± 1.8	28 ± 20
6q		>120	-	
6r		2.7 ± 0.4	-	> 120

a) determinations ± standard deviation (mean of n = 2 unless otherwise stated); b) IC₅₀ mean of n = 4.

Table 9. ERK5 SAR for pyrroles (**39-42**, **44**).

Compound ID	R	ERK5 IC ₅₀ (μM) ^a	
		IMAP	LANCE
39	CH ₃	>120	-
40		3.1 ± 0.1 ^b	-
41		23 ± 4.4	24 ± 2.2
42		6.8 ± 2.0	16 ± 5.7 ^c
44		>120	-

a) determinations ± standard deviation (mean of n = 2 unless otherwise stated); b) mean of n = 4; c) mean of n = 6

FIGURES

Figure 1: Crystal structure of 3-(pyrrolidin-1-ylsulfonyl)-4-thiocyanatobenzenamine **12a**.

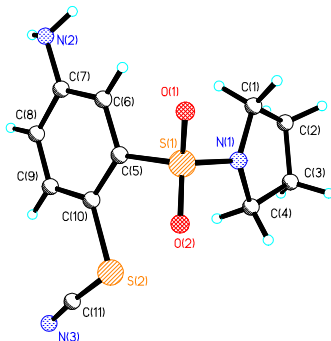


Figure 2: Crystal structure of 6-(pyrrolidine-1-sulfonyl)-benzothiazol-2-ylamine **3a**.

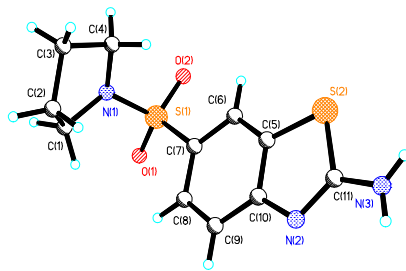
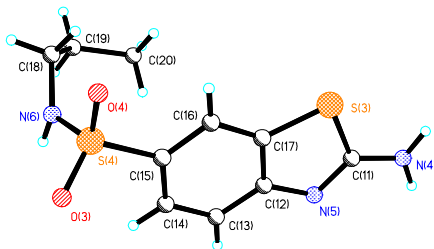
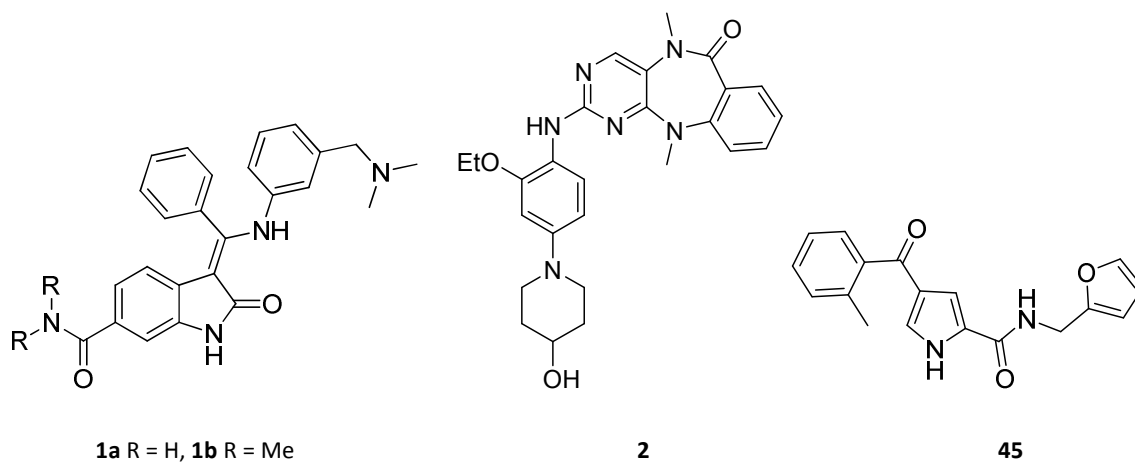


Figure 3: Crystal structure of 2-amino-*N*-propylbenzo[*d*]thiazole-6-sulfonamide **3i**.

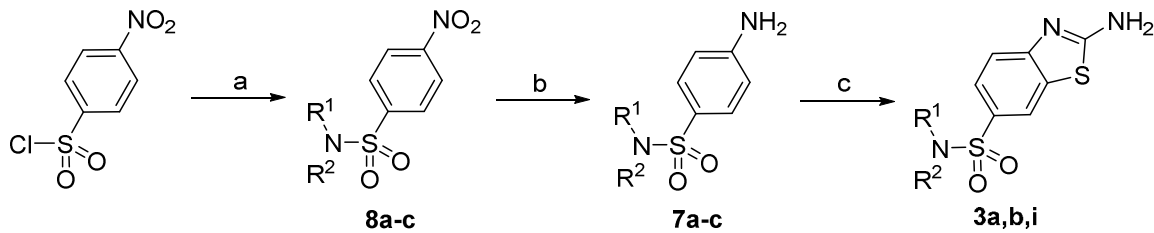


STRUCTURES



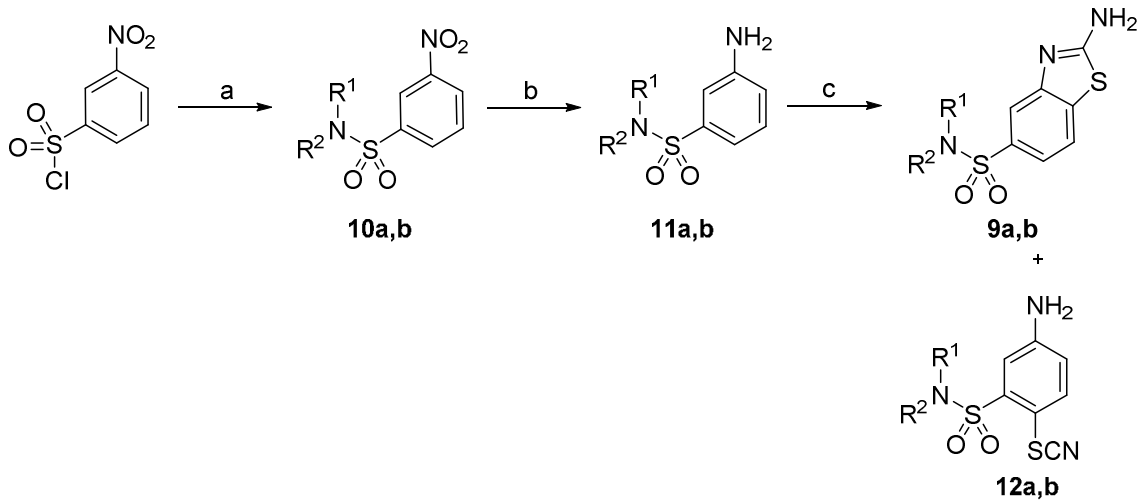
SCHMES

Scheme 1.



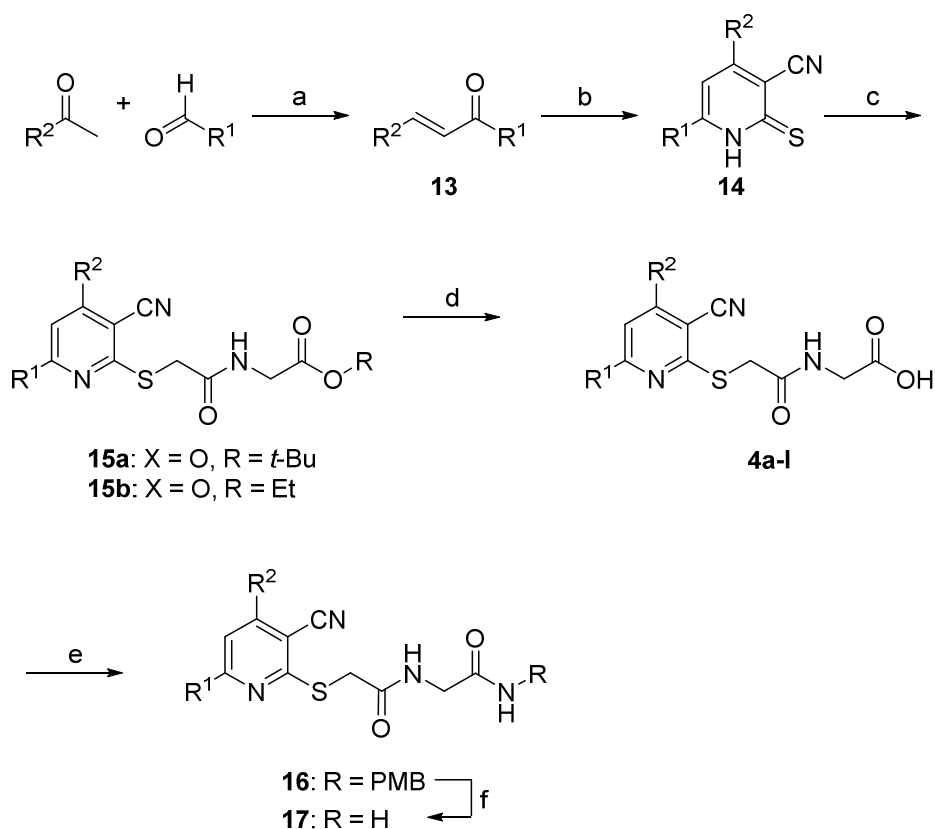
Reagents and conditions: a) pyrrolidine or *N*-methylethylamine or propylamine, Et₃N, DCM; b) Pd/C, H₂, EtOAc; c) KSCN, Cu(II)SO₄, MeOH.

Scheme 2.



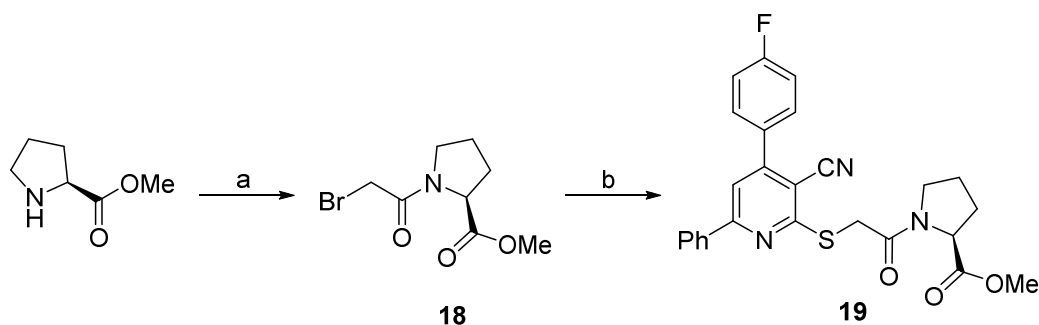
Reagents and conditions: a) pyrrolidine or *N*-methylethylamine, Et₃N, DCM; b) Pd/C, H₂, EtOAc; c) KSCN, Cu(II)SO₄, MeOH.

Scheme 3



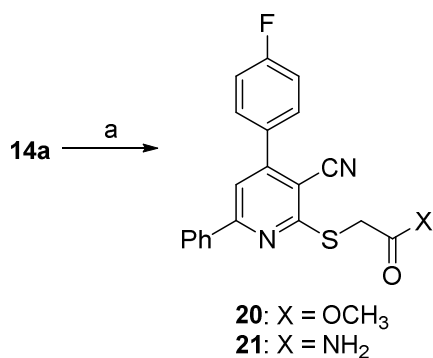
Reagents and Conditions: a) KOH, EtOH, RT; b) Method A, S₈, morpholine, EtOH, 80 °C 30 min then malononitrile; or Method B, 2-cyanothioacetamide, 1.6 M NaOMe in MeOH, 80 °C; c) *tert*-butyl or ethyl 2-(2-bromoacetamido)acetate, K₂CO₃ or KOH, DMF, 100 °C; d) TFA, RT; e) *p*-methoxybenzylamine, HBTU, DIPEA, DMF, 60 °C; f) TFA, 70 °C. NB: No base was required in step c after step b (Method B), as an excess of NaOMe was used in step b

Scheme 4



Reagents and Conditions: a) bromoacetyl chloride, CaCO₃, CHCl₃, H₂O, 0 °C; b) **14a**, KOH, DMF, reflux.

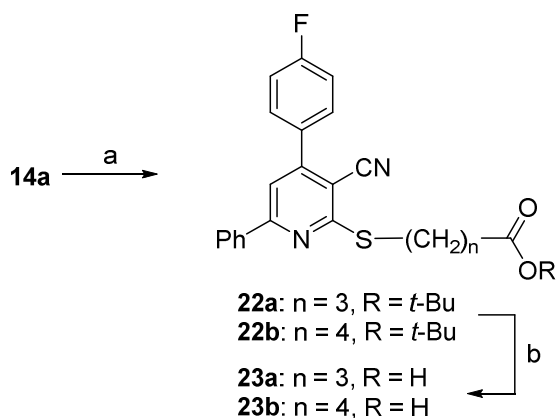
Scheme 5



15
16
17
18
19

Reagents and Conditions: a) methyl bromoacetate, KOH, DMF, reflux, or chloroacetamide, NaOAc.3H₂O, ethanol, reflux.

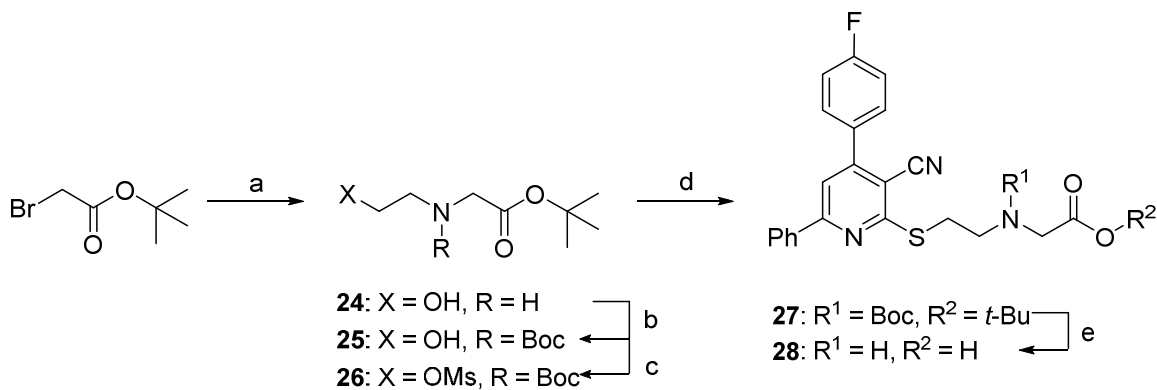
Scheme 6



36
37
38

Reagents and Conditions: a) RBr, K₂CO₃, THF, 100 °C; b) TFA, RT.

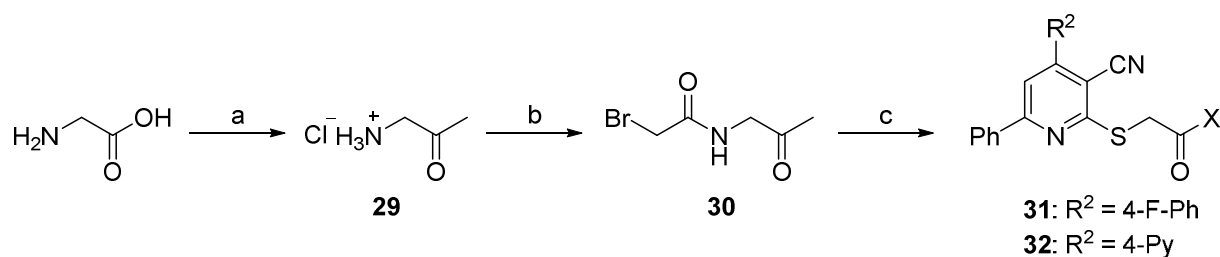
Scheme 7



55
56
57
58
59
60

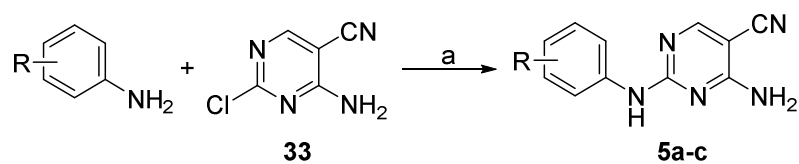
Reagents and Conditions: a) ethanolamine, RT; b) Boc₂O, Et₃N, DCM, 0 °C-RT; c) MsCl, Et₃N, DCM, 0 °C-RT; d) **14a**, DMF, 100 °C; e) TFA, RT.

Scheme 8



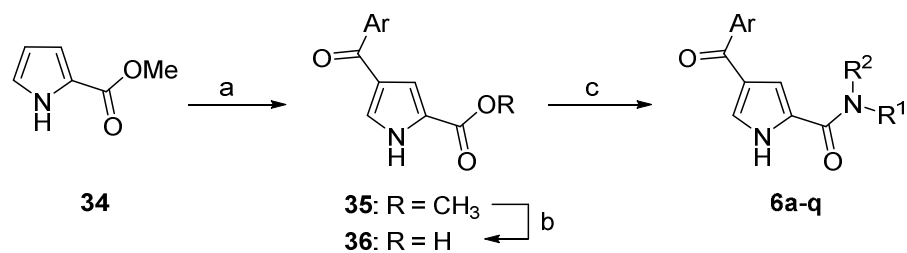
Reagents and Conditions: a) i) Ac₂O, pyridine, reflux; ii) HCl, H₂O, reflux; b) bromoacetyl chloride, CaCO₃, DCM, reflux; c) **14a** or **14g**, K₂CO₃, DMF, 100 °C

Scheme 9



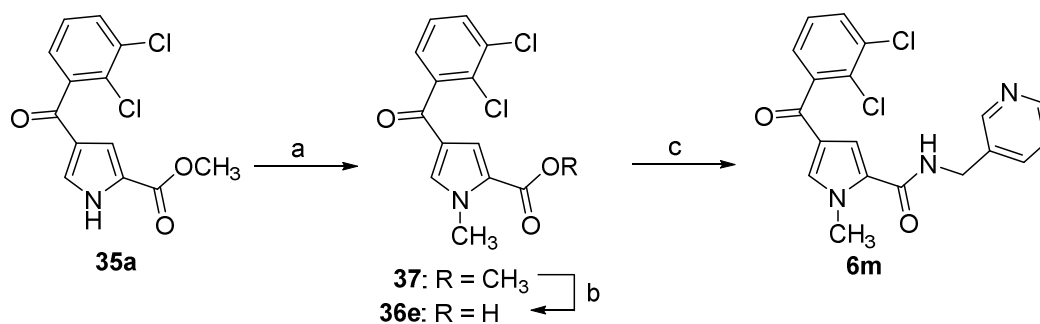
Reagents and Conditions: a) DMF, 100 °C.

Scheme 10



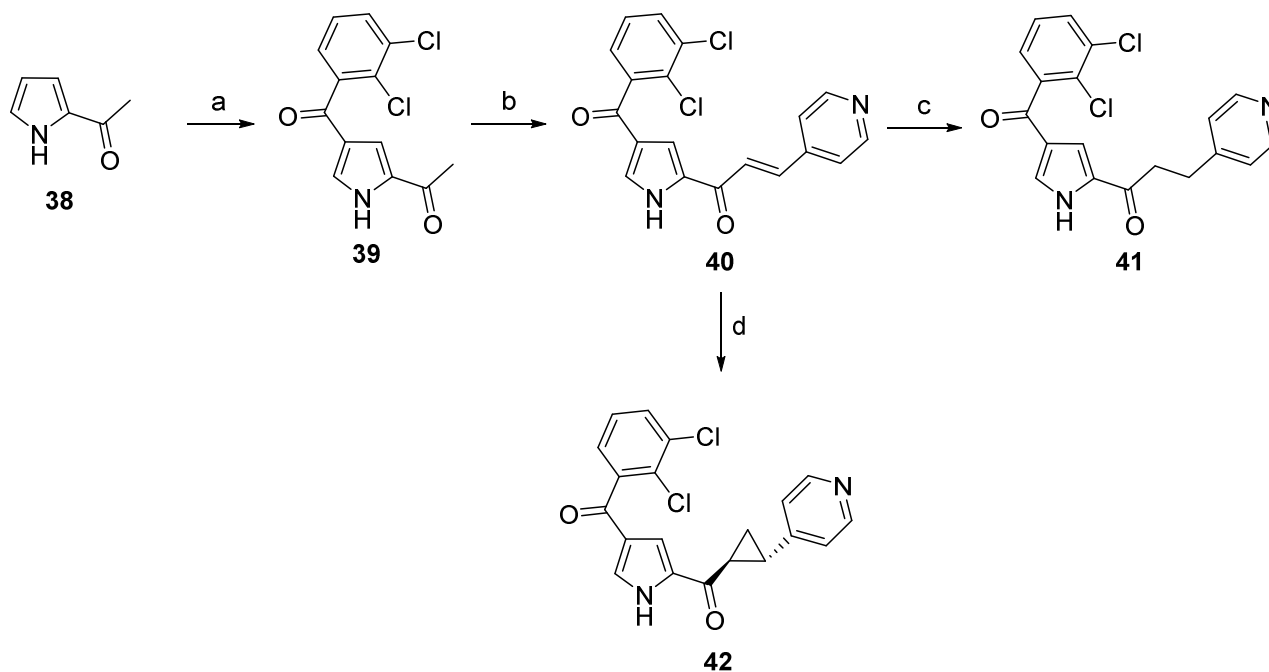
Reagents and Conditions: a) ArCOCl, AlCl₃, DCM, 0 °C-RT; b) LiOH, THF, H₂O, 60 °C; c) i) CDI, THF, 70 °C; ii) R¹R²NH, 50 °C - RT.

Scheme 11



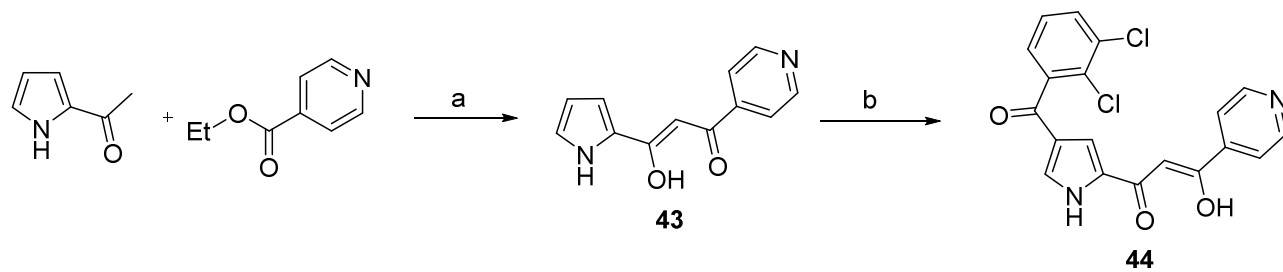
Reagents and Conditions: a) NaH, DMF, MeI; b) LiOH, THF, H₂O, 60 °C; c) i) CDI, THF, 70 °C; ii) 3-pyridylmethylamine, 50 °C - RT.

Scheme 12



Reagents and Conditions: a) AlCl₃, 2,3-dichlorobenzoyl chloride, DCM, 0 °C-RT, 18 h.; b) Isonicotinaldehyde, KOH, EtOH, H₂O, 0 °C-RT, 18 h.; c) Indium powder, NH₄Cl, EtOH, H₂O, reflux, 8 h; d) (CH₃)₂SO⁺I⁻, KO^tBu, DMSO, RT, 24 h.

Scheme 13



Reagents and Conditions: a) KO^tBu , THF, RT, 6 h. b) AlCl_3 , 2,3-dichlorobenzoyl chloride, DCM, 0 °C-RT, 18 h.

TOC graphic

